



## OPEN ACCESS

## EDITED BY

Diego Raimondo,  
University of Bologna, Italy

## REVIEWED BY

Daniele Neola,  
University of Naples Federico II, Italy  
Ying Qin,  
Dongguan Maternal and Child Health  
Hospital, China

## \*CORRESPONDENCE

Kana Wang

✉ kanawishes@163.com

RECEIVED 18 June 2024

ACCEPTED 24 February 2025

PUBLISHED 17 March 2025

## CITATION

Yuan M, Chen S, Liao Z and Wang K (2025)  
The expression of autophagy-related gene  
CXCL12 in endometriosis associated ovarian  
cancer and pan-cancer analysis.  
*Front. Endocrinol.* 16:1450892.  
doi: 10.3389/fendo.2025.1450892

## COPYRIGHT

© 2025 Yuan, Chen, Liao and Wang. This is an  
open-access article distributed under the terms  
of the [Creative Commons Attribution License  
\(CC BY\)](#). The use, distribution or reproduction  
in other forums is permitted, provided the  
original author(s) and the copyright owner(s)  
are credited and that the original publication  
in this journal is cited, in accordance with  
accepted academic practice. No use,  
distribution or reproduction is permitted  
which does not comply with these terms.

# The expression of autophagy-related gene CXCL12 in endometriosis associated ovarian cancer and pan-cancer analysis

Mingwei Yuan<sup>1,2</sup>, Sijing Chen<sup>1,2</sup>, Zelan Liao<sup>1,2</sup> and Kana Wang<sup>1,2\*</sup>

<sup>1</sup>Department of Obstetrics and Gynecology, West China Second University Hospital, Sichuan University, Chengdu, China, <sup>2</sup>Key Laboratory of Birth Defects and Related Diseases of Women and Children (Sichuan University), Ministry of Education, Chengdu, China

**Background:** Endometriosis-associated ovarian cancer (EAOC), an aggressive form of malignant ovarian neoplasm with origins in endometriosis (EM), has risen to prominence recently. Despite extensive investigation, the precise pathophysiology remains elusive. This article explores new autophagy-related DEG genes between EM and EAOC, and investigates CXCL12's expression and prognostic relevance across pan-cancer.

**Methods:** From Gene Expression Omnibus (GEO), we retrieved gene sequencing data to uncover DEGs. We carried out enrichment analysis, PPI network construction and explored CXCL12's multi-database expression and prognostic significance employing the analytical tools of ONCOMINE, PrognoScan, GEPIA, and Kaplan-Meier Plotter. Subsequently, assessing the relationship between CXCL12 expression and immune presence in cancer utilizing GEPIA and TIMER. Lastly, CXCL12, IL17, STAT3, and FOXP3 protein expressions were determined through immunohistochemistry analysis in EAOC, EM, and normal endometrial tissues.

**Results:** Two DEGs were discovered and enrichment analysis indicated virus-cytokine/receptor interactions, chemokine signaling, and cytokine-cytokine receptor interplay as pivotal in EAOC. Notably, cancerous tissues exhibited reduced CXCL12 levels compared with non-malignant tissues across cancers. CXCL12, IL17, STAT3, Th17/Treg ratio, and FOXP3 expressions were also lower in EAOC than EM and normal tissues. Additionally, CXCL12 expression was related to stage, survival, immune subtype, and molecular classification across cancers.

**Conclusions:** In conclusion, our study implicates CXCL12 and altered Th17/Treg balance in progression from EM to EAOC. CXCL12 emerges as a predictive marker for cancer progression across various tumors and is associated with inflammatory response.

## KEYWORDS

endometriosis-associated ovarian cancer, autophagy, integrated bioinformatics approaches, pan-cancer, survival analysis, immune infiltration

## Introduction

Endometriosis (EM), an imposing gynecologic disorder, affects approximately 5%-20% of women in childbearing years (1–3). Among those experiencing pelvic pain and infertility, EM prevalence rises to a shocking 30%-50% (4, 5). Its manifestations include tumors, pain, and infertility, severely impacting quality of life and fertility. Like malignant tumors, EM displays traits of invasiveness, adhesivity, and metastasis, heightening concerns about its cancerous potential. In 1925, Sampson first linked EM with ovarian cancer, establishing the diagnostic criteria for Endometriosis Associated Ovarian Cancer (EAOC). These include coexistence of EM and cancer tissue within a lesion, histological correlation between both, and exclusion of other primary tumors. In 1953, ScoR refined these guidelines further, adding histological evidence of EM transition towards malignancy (6). Numerous studies establish stronger links among EM and ovarian cancer, increasing risk of ovarian cancer up to 1.265-2.14 times for EM patients (7, 8), specifically for ovarian clear cell carcinoma (OCCC) and ovarian endometrioid adenocarcinoma (OEC) (9). This risk persists even postmenopausal and EM symptom resolution (10), notably, CKD(chronic kidney disease)history exceeding ten years or primary infertility augments this risk, respectively 2.51 times and 2.72 times higher than non-EM secondary infertility patients (11, 12).

The mechanism of EM evolving into EAOC remains unclear, potentially linked to microenvironmental factors like immune and inflammation responses, excess estrogen, oxidative stress, or specific gene mutations and alterations such as ARID1A, PTEN, PIK3CA and KRAS) (13–17). Autophagy, a highly conserved metabolic process in eukaryotes, plays pivotal roles in stress response and maintaining cellular homeostasis (18). It not only influences the progression of endometriosis (19) but potentially contributes to ovarian cancer through cell behavior changes like drug resistance, dormancy, and stemness maintenance (20).

Consequently, exploring autophagy's effects on ovarian cancer related to endometriosis is crucial for understanding this correlation and developing novel therapeutic strategies.

## Materials and methods

### Data sources

Utilizing the Gene Expression Omnibus (GEO) genomic database (<http://www.ncbi.nlm.nih.gov/geo>), keyword searches for “endometriosis” and “endometriosis-associated ovarian cancer” identified two gene expression datasets meeting our selection criteria: GSE57545 and GSE157153. These datasets were sourced from GPL18671 and GPL17303 platforms respectively (21, 22).

### Selection of differentially expressed genes

NetworkAnalyst (<https://www.networkanalyst.ca/NetworkAnalyst/faces/home.xhtml>) was utilized for differential expression gene (DEG) assessment in comparing nonmalignant endometriosis and

endometrioma-associated ovarian carcinoma tissue (23). Genes exhibiting an adjusted P-value <0.05 and a log fold change ( $|\log_{2}FC|$ ) >1 were deemed DEGs. The Autophagy Database HAMdb2 (<http://hamdb.scbdd.com/home/index/>) was employed (24), cross-referencing with datasets GSE57545 and GSE157153 to identify autophagy-linked DEGs. The ggplot2 (version 3.3.6) package within R software was utilized to plot the DEG volcano plot. Online tool Funrich (<http://funrich.org/>) generated the DEG Venn diagram (25).

### Construction of protein-protein interaction networks and GO/KEGG analysis

GeneMANIA (<http://www.genemania.org>), a database for elucidating protein-protein interaction (PPI) networks, was employed to construct networks encompassing functionally correlated genes from existing genomics and proteomics datasets (26). Gene functional analysis by GO, KEGG enrichment scrutiny was conducted on genes closely connected to CXCL12, sourced from STRING utilizing the “clusterProfiler” and “org.Hs.eg.db” packages in R (27). GO and KEGG pathway enrichments were performed with a p-value threshold of <0.01, showing outcomes in a ggplot2 bubble chart format.

### Differential expression analysis of CXCL12

Data comprising 11,315 cancerous tissue and matched healthy counterparts from TCGA (<https://www.cancer.gov/aboutnci/organization/ccg/research/structural-genomics/tcga>) and mRNA patterns in 31 GTEx (<https://commonfund.nih.gov/GTEx>) derived tissues were utilized. We assessed CXCL12 expression levels across these 31 normal and 33 cancer tissues and compared them against their matched controls. Significance testing using log<sub>2</sub> transformation and t-tests revealed expression variances significant at a p-value lower than 0.05. Data processing tasks were executed via R software (version 4.2.1, <https://www.Rproject.org>), incorporating the “ggplot2” package for graphical representation.

### Immunohistochemistry staining of CXCL12

CXCL12 protein quantification was accessed through the CPTAC database via UALCAN (<http://ualcan.path.uab.edu/>) (28). The Human Protein Atlas (<https://www.proteinatlas.org/>), a comprehensive database, catalogs protein distributions in human tissues and cells (29). Evaluating CXCL12 protein expression, we accessed immunohistochemistry data obtained from HPA's repository of 15 tumor and matched normal tissue specimens.

### Analysis of the diagnosis value of CXCL12

ROC analysis on CXCL12 in 33 cancers evaluated its applicability as a diagnostic tool. mRNA expressions of CXCL12

in TCGA and GTEx somatic tumors and their corresponding adjacent healthy tissue were utilized for these assessments. ROC curves were developed using R's "pROC" package (v1.17.0.1). Additionally, area under curve (AUC), cutoffs, sensitivities, specificities, positive predictive values, negative predictive values, and Youden's index (YI) were calculated. An elevated AUC reflects superior diagnostic capability. An AUC between 0.5 and 0.7 denotes poor accuracy, 0.7 to 0.9 marks fair accuracy, with an AUC of 0.9 or above signifying stellar accuracy. High YIs indicate more effective patient-screening methods (30, 31).

## Analysis of the relationships between CXCL12 and prognosis

Accessing TCGA downloads enabled us to explore correlations between CXCL12 expression and patient outcomes: overall survival (OS), disease-specific survival (DSS), and progression-free interval (PFI). For survival analysis per cancer type, the Kaplan–Meier method and log-rank test were utilized. We leveraged R packages "survival" and "survminer" for visualization of survival curves. Additionally, "forestplot" was used to determine the pan-cancer association between CXCL12 expression and survival.

## CXCL12 expression in different molecular and immune subtypes of cancers

Investigating associations between CXCL12 expression and subtype classifications within 33 cancers entailed utilization of the "subtype" module of TISIDB, a comprehensive resource that integrates diverse datasets related to tumor-immune system interplay (32). Investigated CXCL12 mRNA expression among unique immunological subtypes: C1 (wound healing), C2 (IFN-g dominant), C3 (inflammatory), C4 (lymphocyte deplete), C5 (immunologically quiet), and C6 (TGF- $\beta$  dominant).

## Analysis of the promoter methylation of CXCL12

UALCAN (<http://ualcan.path.uab.edu/>), a comprehensive web interface, facilitated in-depth transcription factor (TF) deregulation evaluation of TCGA gene expression profiles. This research application utilized UALCAN to scrutinize promoter methylation status of the chemokine CXCL12 across diverse cancer types.

## The gene set cancer analysis

The GSCALite platform (<http://bioinfo.life.hust.edu.cn/web/GSCALite/>) synthesizes genomic data on 33 cancers from TCGA with drug response data from GDSC, CTRP, along with GTEx's normal tissue info, for streamlined gene set evaluation (33). Utilizing this platform, we examined the alterations to well-known cancer-

involved pathways in the 33 cancer variations of CXCL12, specifically focusing on TSC/mTOR, RTK, RAS/MAPK, PI3K/AKT, ER, AR, EMT, DDR, Cell Cycle, and Apoptosis pathways.

## Relationship between CXCL12 expression and immunity

CIBERSORT, an agnostic metagenomic tool, derived relative expression scores for 24 immunity cells in 33 tumor samples to define their immunocyte phenotype. Moreover, R "ggplot2" and "ggpubr" packages determined correlation coefficients between CXCL12 and infiltrating immune subset levels. Additionally, co-expression profiles of CXCL12 with immunity-associated genes coding for MHC, immune activation, suppression, chemokines, and receptors, were evaluated.

## Correlation of CXCL12 expression with DNA methylation

UALCAN (<http://ualcan.path.uab.edu/>) serves as an interactive web portal enabling extensive analysis of TCGA gene expression data. Utilizing UALCAN, this investigation examined the promoter methylation status of CXCL12 across diverse cancer types. cBioPortal (<http://www.cbioportal.org/>), a comprehensive resource that incorporates TCGA's tumor gene datasets, provides researchers with multi-dimensional data visualization (34). Utilizing cBioPortal, we mined data from 32 cancers comprising 10,953 samples for further investigation. On "OncoPrint" and "Cancer Type Summaries", we explored mutations in the CXCL12 gene across various tumor types and their profiling. "OncoPrint" displayed the target gene's mutation, copy number, and expression patterns via heat maps, while "Cancer Type Summaries" illustrated the gene's mutation rates in general carcinomas through bar charts.

## Immunogenomic analyses of CXCL12 in the 33 cancers

The GSVA module coupled with ssGSEA analytics investigated the link between CXCL12 expression and tumor infiltrating lymphocytes, immunomodulators, suppressors, MHC molecules, chemokines, and their respective receptors across 33 cancers. This analysis utilized Spearman's rank correlation method; p-values below 0.05 were designated as statistically significant. Subsequently, ggplot2 package generated heatmap visualizations.

## Immunohistochemistry of 54 clinical cases

We procured FFPE archives from 26 EAOE tissues, 10 EM, and 18 control endometrial tissues at the West China Secondary Hospital. The procedure involved deparaffination, dehydration, citrate buffer antigen retrieval via microwave, 3% H<sub>2</sub>O<sub>2</sub>

treatment, and overnight incubation with anti-human CXCL12, IL17, STAT3, FOXP3 antibodies (Proteintech, Wuhan, China). Next, the sections were incubated with secondary antibody at room temperature for 2 hours. DAB kit (Solarbio, Beijing, China, DA-1010) was employed for color development. Randomly selected fields were observed under microscope, scoring the intensity of positive cells on a scale of 0-3 (0 = faint; 3 = strong), and the staining extent as follows: 0 = < 5%; 1 = 5-25%; 2 = 26-50%; 3 = 51-75%; 4 = 76-100%. The final IHC staining score was obtained by multiplying these two values, defining positivity as a score > 2.

## Results

### Identification of differentially expressed genes associated with autophagy DEG

GSE57545 dataset obtained 130 differentially expressed genes, including 117 up-regulated genes and 13 down-regulated genes, and GSE157153 dataset obtained 3824 differentially genes including 1350 up-regulated genes and 2474 down-regulated genes. Two gene products were identified after intersecting the DEGs in GSE57545, GSE157153, and autophagy-associated genes, and we selected CXCL12 as the differentially expressed genes of autophagy-related genes and further analyzed it as key gene (Figure 1).

### Expression landscape of CXCL12

Remarkably, CXCL12 exhibited elevated expression in adipose, endometrial, spleen, and smooth muscle tissues, whereas placental and cerebral cortex showed reduced levels (Figure 2).

### Pan-cancer mRNA expression of CXCL12

Results indicated reduced CXCL12 levels in tumor compared to their respective control tissues, including BLCA, BRCA, CESC,

CHOL, COAD, ESCA, HNSC, KICH, KILC, KILP, LIHC, LUAD, LUSC, PRAD, READ, STAD, THCA, UCEC, ACC, OV, SKCM, UCS. It was increased in DLBC, LAML, LGG, TGCT. When comparing GBM, PAAD, PCPG and their normal tissues, there were no significant differences in CXCL12 gene expression levels. Among the paired sample analyses, CXCL12 mRNA expression was decreased in BLCA, BRCA, CHOL, COAD, HNSC, KICH, KIRC, KIRP LIHC, LUAD, LUSC, PRAD, READ, STAD, THCA, UCEC. There was no difference shown in CESC, ESCA, PAAD, PCPG (Figure 3).

### Pan-cancer protein expression of CXCL12

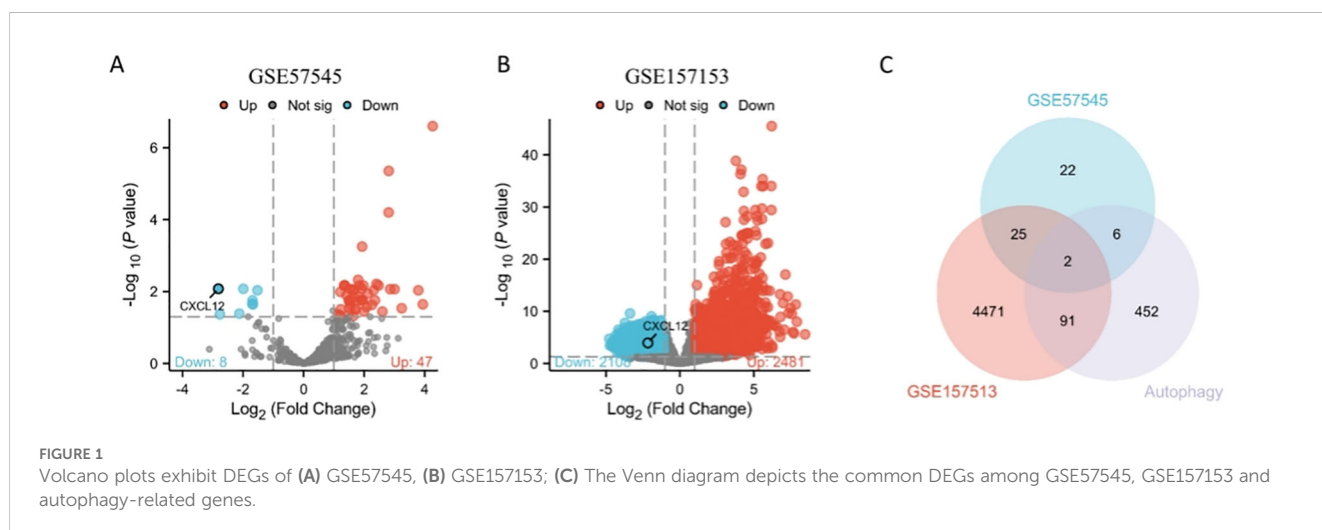
The CXCL12 protein expression is reduced in LUAD, UCEC, BRCA, KIRC, OV, LIHC, COAD, PAAD, HNSC compared to normal tissue (Figure 4).

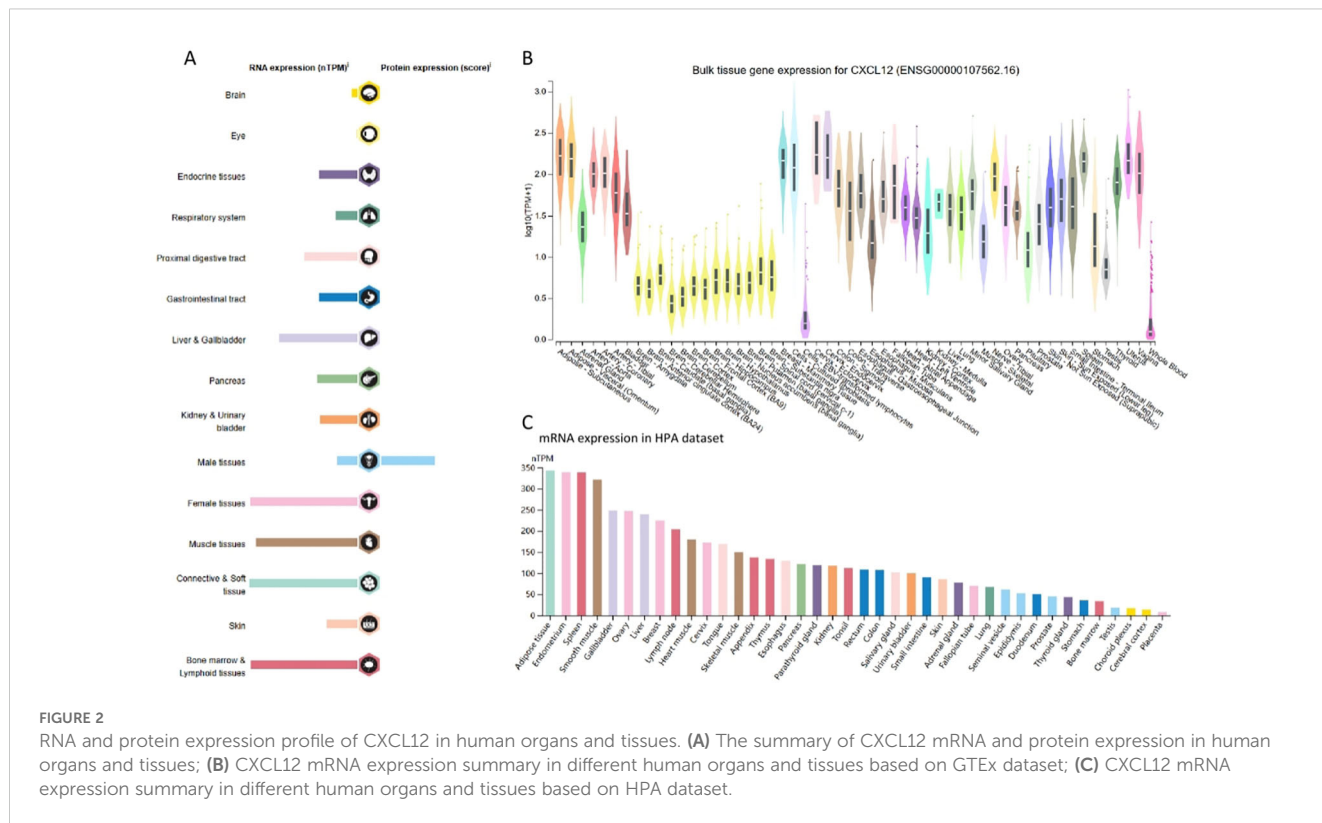
### The expression of CXCL12 in different stage

CXCL12 expression reduces in initial stages of tumor during our study on its staging correlation, including BLCA, STAD, LUAD, LIHC, COADREAD, CESC, HNSC, BRCA, OV and UCEC indicating that CXCL12 potentially offers substantial clinical utility for diagnosing these tumors at an early stage (Figure 5).

### The diagnostic value of CXCL12 in the 33 cancers ROC

As shown in Figures 6, CXCL12 has a good diagnostic value in a variety of cancers. Its AUC was greater than 0.7 in 13 cancers and even exceeded 0.9 in 7 cancers including CESC (AUC = 1), BLCA (AUC = 0.907), LUAD (AUC = 0.912), LIHC (AUC = 0.932), COADREAD (AUC = 0.964), UCEC (AUC = 0.953), BRCA (AUC = 0.944), PAAD (AUC = 0.715), STAD (AUC =





0.703), SKCM (AUC = 0.737), THCA (AUC = 0.866), OSCC(AUC = 0.722), OV (AUC = 0.779), ESCA (AUC = 0.626),CHOL(AUC = 0.692),HNSC (AUC = 0.697),PRAD (AUC = 0.688) (Figure 6).

OV (four subtypes), PAAD (five subtypes), UVM (three subtypes), PCPG (five subtypes), PRAD (four subtypes), SARC (five subtypes), SKCM (five subtypes), STAD (five subtypes), tgct (four subtypes), THCA (five subtypes), UCEC (five subtypes) (Figure 9).

### Survival analysis of CXCL12 in the 33 cancers OS

The results suggest that for BLCA's 33 cancers, CXCL12 acts as a significant risk factor for DSS. The result found that high CXCL12 groups have statistically better OS than those for the low CXCL12 groups in CCSK, LUAD, LIHC, LARC, CESE. However, the low CXCL12 groups show statistically better OS than high CXCL12 groups in BLCA, STAD, KIRP, LUSC, OV (Figure 7).

### CXCL12 expression in different immune and molecular subtypes of the 33 cancers

For molecular subtypes, CXCL12 expresses significantly differently in 13 cancer types, including ACC, BRCA, GBM, HNSC, KIRP, LIHC, LUSC, OV, PCPG, STAD, UCEC, LGG, PRAD (Figure 8). Results indicate significant divergence between immune subtypes in ACC (six subtypes), BLCA (six subtypes), BRCA (six subtypes), CESC (three subtypes), ESCA (six subtypes), GBM (three subtypes), HNSC (six subtypes), KICH (four subtypes), KILC (six subtypes), KIRP (six subtypes), LGG (four subtypes), LICH (five subtypes), LUAD (five subtypes), lusc (five subtypes),

### Genetic mutations of CXCL12

A total of 17 sites from amino acid positions 0 to 93 exhibited mutation activity, including 13 missense, two truncation, one splice, one fusion (SV) and most predominantly, K75E/T (Missense). The predominant mutation categories identified included Missense, Amplification, and Deep Deletion. Notably, CXCL12's gene alteration across various tumor tissues was assessed using this platform; amplifications being the most prevalent. Mutations of CXCL12 notably occurred more frequently in HNSC and UCEC. Deep deletions were prevalent in PRAC, Sarcoma, and BRAC among the 32 cancers examined. Furthermore, an investigation into the correlation between CXCL12 genetic alternations and clinical survival outcomes in ovarian cancer revealed poorer prognoses amongst patients with altered CXCL12 (Figure 10).

### Promoter methylation levels of CXCL12

Figure 11 illustrates elevated CXCL12 promoter methylation in 17 tumor groups compared to controls (Figure 11).

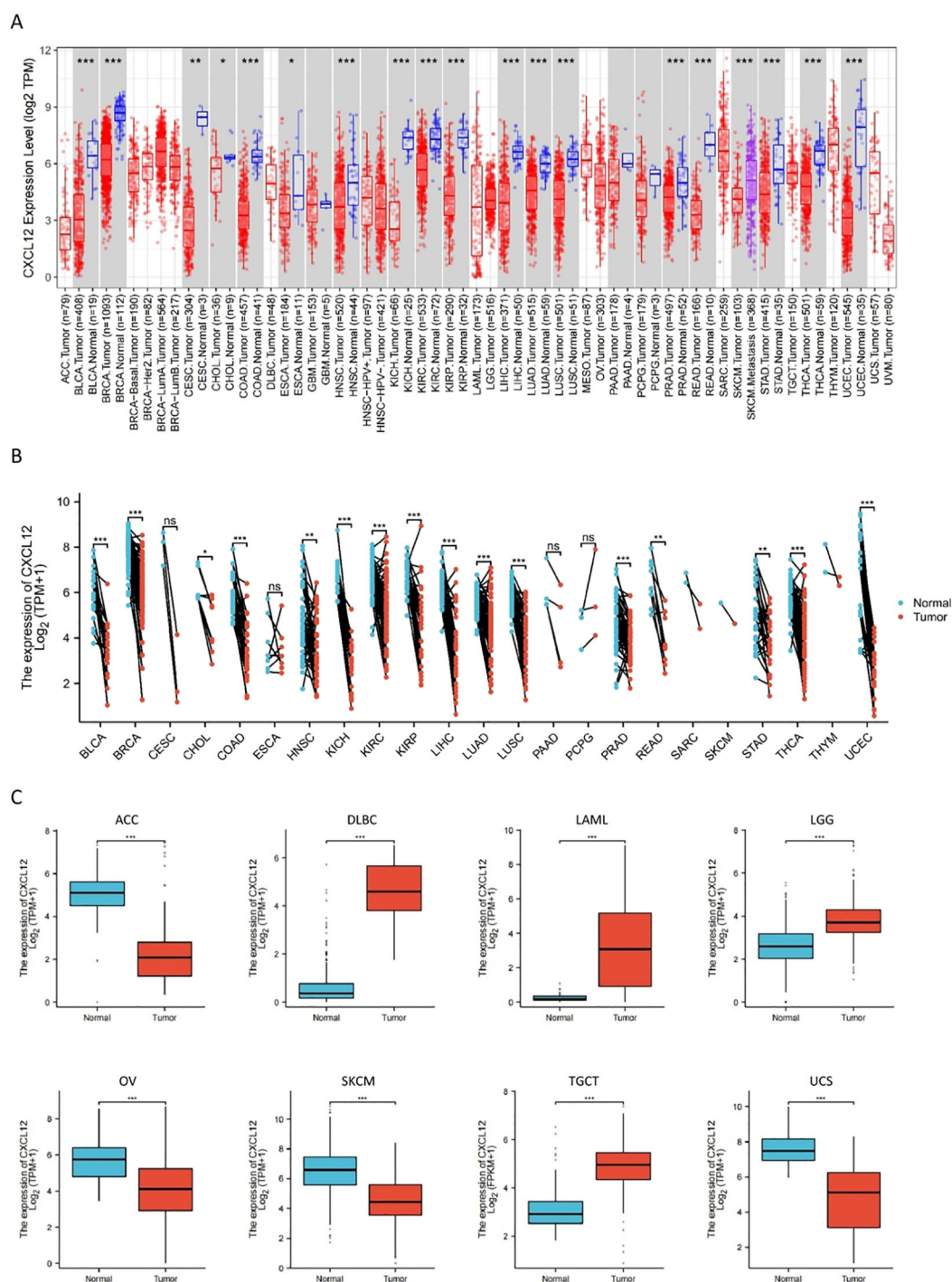


**FIGURE 3** Expression of CXCL12 mRNA in pan-cancer. (A) Expression of CXCL12 between the 33 cancers and normal tissues in unpaired sample analysis; (B) Expression of CXCL12 between the 33 cancers and normal tissues in paired sample analysis; (C) Paired sample analysis of CXCL12 mRNA expression between 8 cancers and normal tissues in ACC, DLBC, LAML, LGG, OV, SKCM, TGCT and UCS. (\* $p < 0.05$ , \*\* $p < 0.01$ , \*\*\* $p < 0.001$ , ns, Not Significant).

## The PPI, functional enrichment of CXCL12 in cancers

We identified 21 genes in tight correlation with CXCL12, forming a PPI network. Analysis revealed GO/KEGG enrichments among these

genes. Three major classifications under RNA function include biological process (BP), molecular function (MF), and cellular component (CC). Key GO terms relevant to BP include chemokine signaling pathway, cell response to chemokines, and response to chemokines. For CC, they encompass external side of plasma

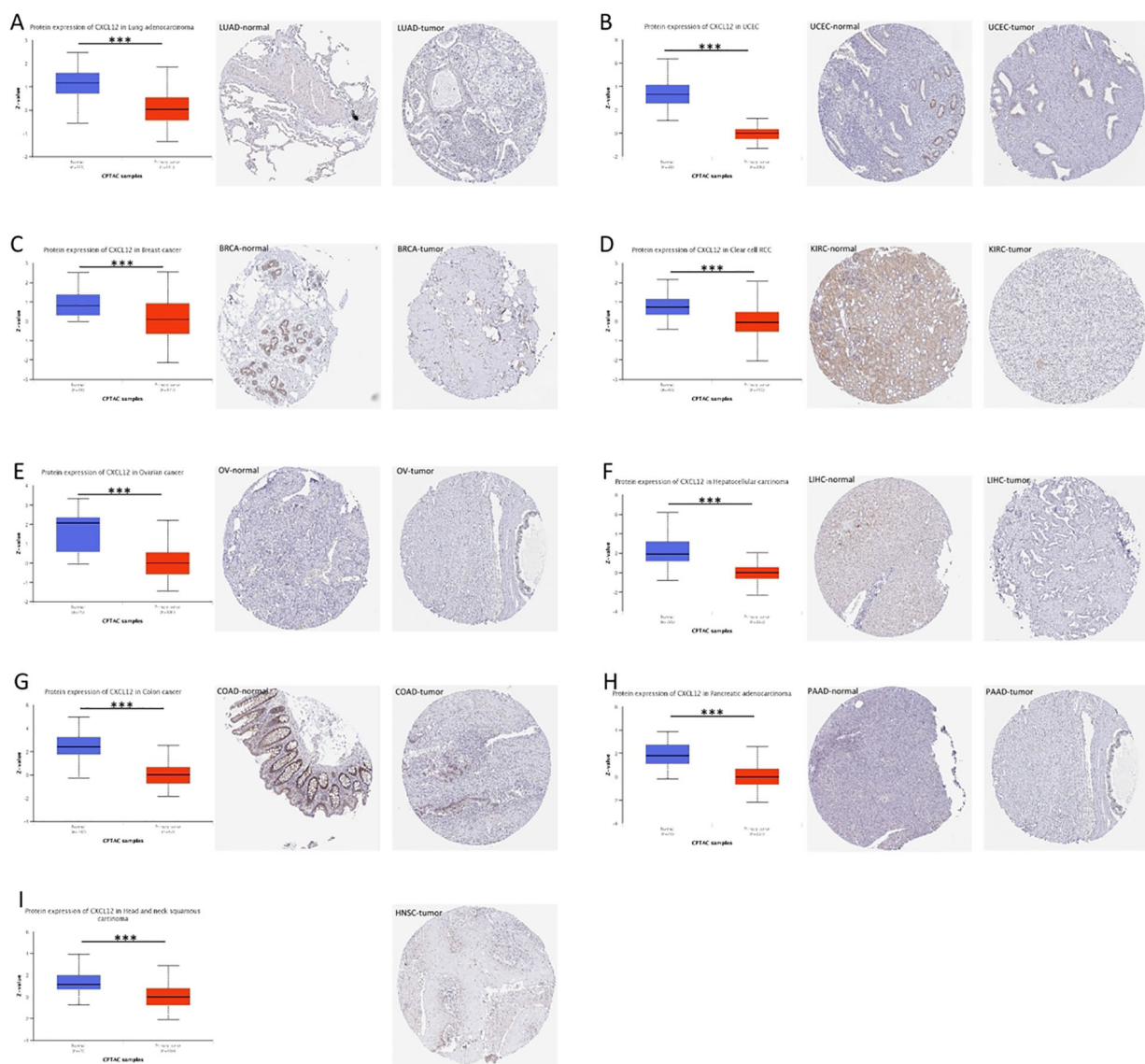


**FIGURE 4** Expression of CXCL12 in tumor tissues and normal tissues of different cancers in TCGA database (left), immunohistochemical image of CXCL12 in normal tissues in HPA database (middle), and immunohistochemical image of CXCL12 in tumor tissues in HPA database (right). (A) LUAD; (B) UCEC; (C) BRCA; (D) KIRC; (E) OV; (F) LIHC; (G) COAD; (H) PAAD; (I) HNSC. (\* $P < 0.05$ , \*\* $P < 0.01$ , \*\*\* $P < 0.001$ ).

membrane, platelet alpha granule lumen, and platelet alpha granule. As for MF, they involve chemokine activity, chemokine receptor binding, and cytokine activity. Top KEGG pathways include Viral protein interaction with cytokine and cytokine receptor, Chemokine signaling pathway, and Cytokine-cytokine receptor interaction. Pathways activated by CXCL12, predominantly in cancer cells, include EMT, hormone ER, PI3K/AKT, RAS/MAPK, RTK, and TSC/mTOR. Conversely, apoptosis, cell cycle, DNA damage, hormone AR, and RTK are suppressed (Figure 12).

### Functional states of CXCL12 in scRNA-Seq datasets

Negative relationships between CXCL12 and key biological processes such as cell cycle, DNA damage/repair, epithelial-to-mesenchymal transition (EMT), hypoxia, invasion, metastasis, proliferation, and quiescence suggested potential tumor suppressor roles for CXCL12. Examining CXCL12's correlation with specific cancer functions revealed positive links with

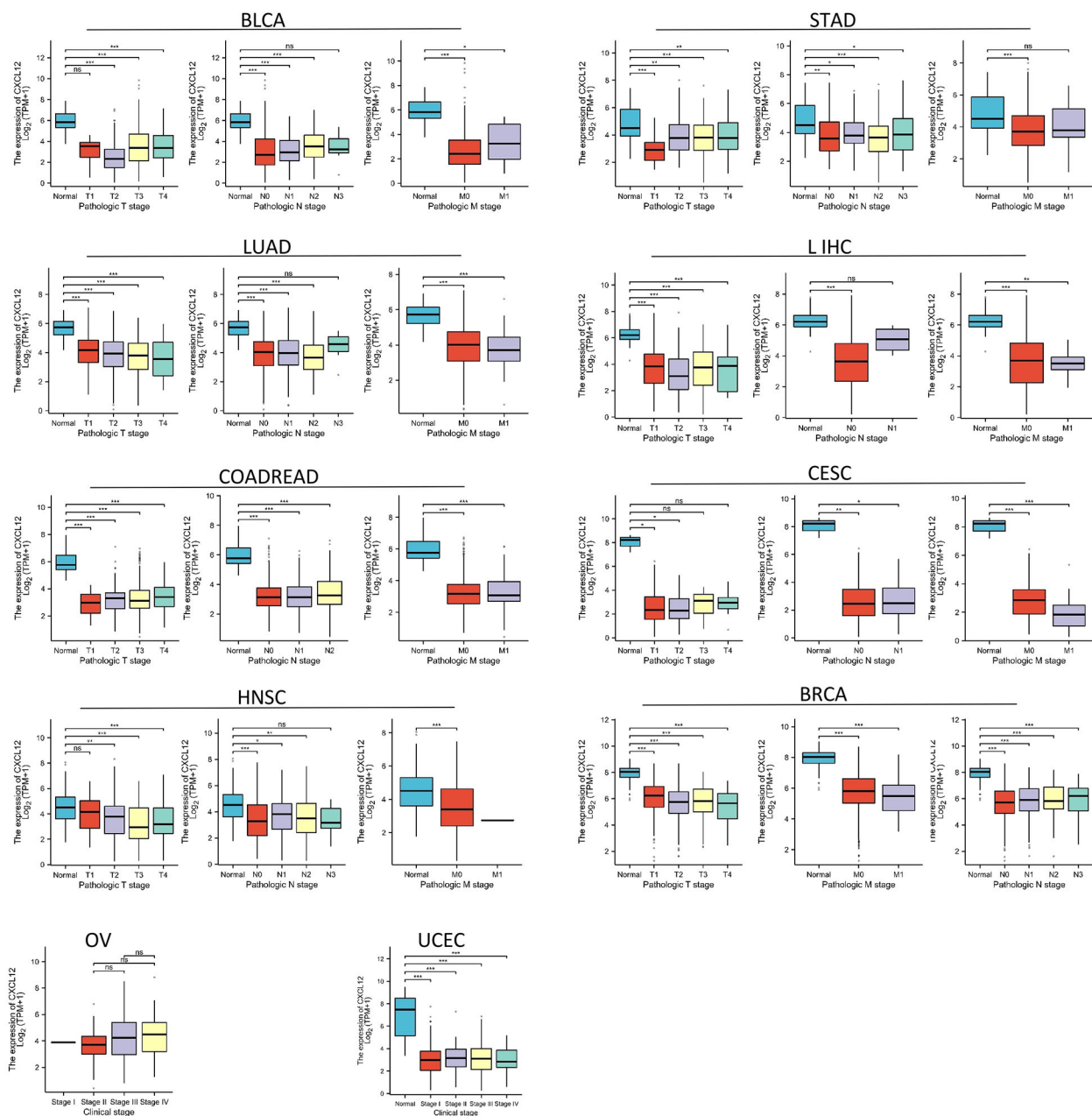


**FIGURE 5**  
Association between CXCL12 expression and tumor stage. (\* $p < 0.05$ , \*\* $p < 0.01$ , \*\*\* $p < 0.001$ . ns, not statistically significant).

inflammation, differentiation, and angiogenesis in retinoblastoma (RB) but negative correlations with DNA repair, DNA damage, and cell cycle. In osteosarcoma (OG), CXCL12 was positively associated with inflammation, metastasis, cell cycle, differentiation, hypoxia, and negatively related to DNA repair, DNA damage, and invasion (Figure 13).

### Immunogenomic analyses of CXCL12 in the 33 cancers

Results indicated a significant positive correlation between CXCL12 and most immune cells across 33 cancers, notably SKCM, KICH, UVM. Notably, CXCL12 displayed a positive correlation with



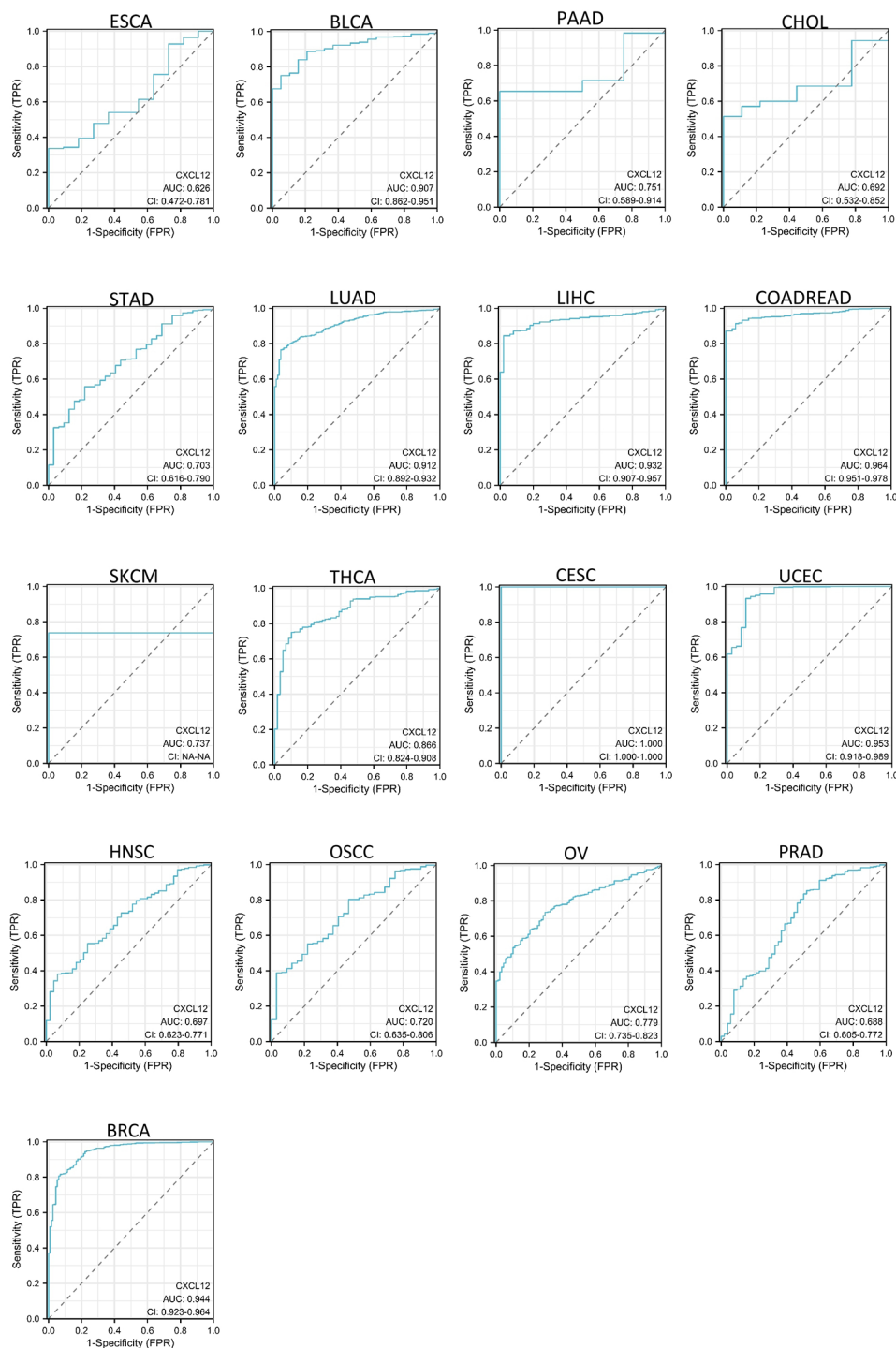
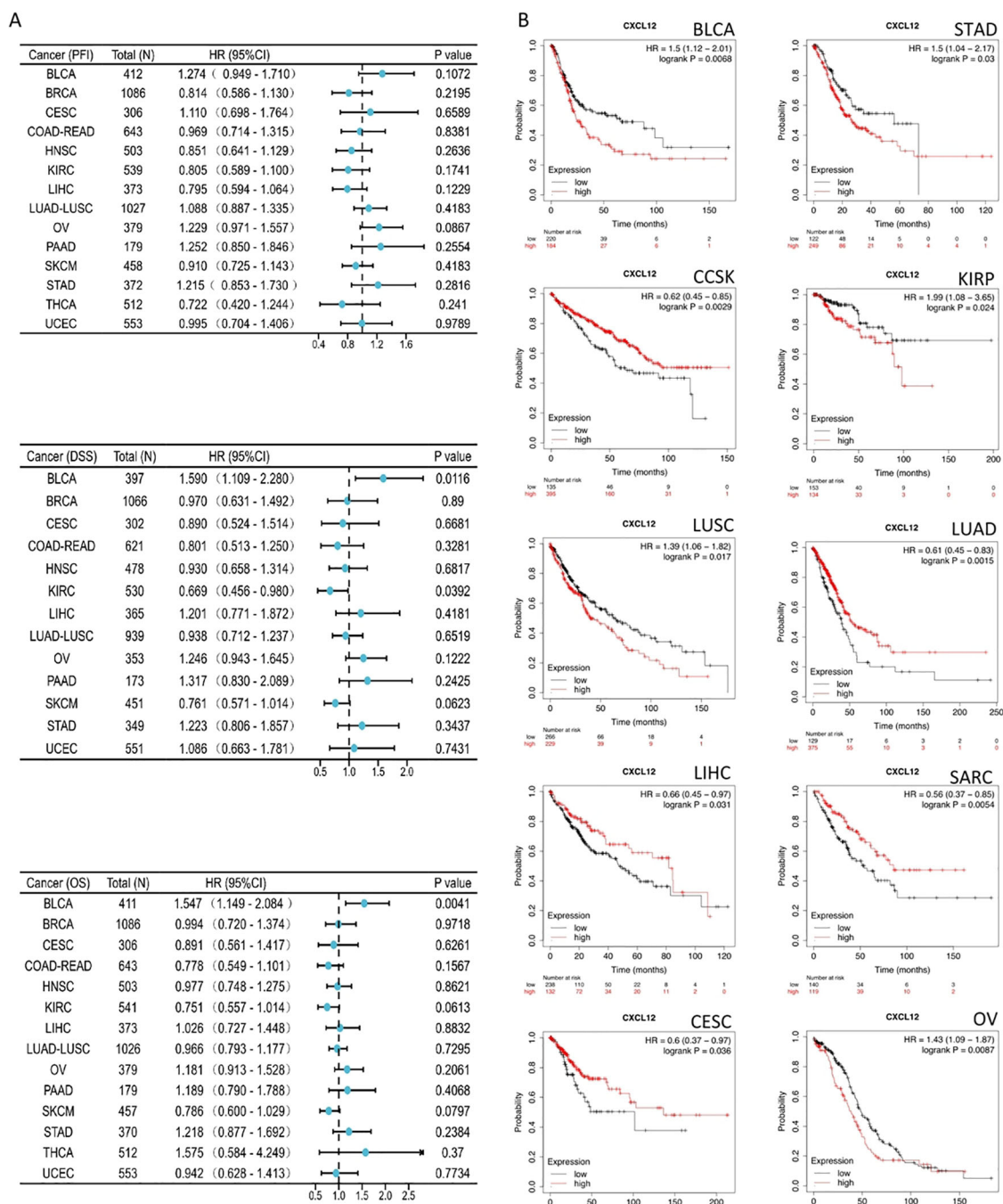


FIGURE 6 AUC of ROC curves verified the diagnosis performance of CXCL12 in the TCGA cohort.

most immunostimulators, excluding KIR2DL1 and KIR2DL3, specifically in HNSC, KIRC, KIRP, LIHC, STAD, THCA, and UVM. A positive correlation with most MHCs was observed in KICH, UVM, SKCM, LUSC, CHOL, while a negative correlation with most MHCs was seen in UCS and STAD. Positive correlations were found between CXCL12 and most cytokines in COAD, KIRC, LGG, LIHC, PRAD, THCA, and UVM. Concerning cytokine receptors,

CXCL12 exhibited a positive correlation with most in HNSC, KIRC, LIHC, PRAD, THCA. Utilizing TIMER, CIBERSORT, CIBERSORT-ABS, QUANTISEQ, XCELL, MCPOUNTER, and EPIC algorithms, we examined the potential link between CXCL12 expression and immune cell infiltration in various TCGA cancer types. Analysis revealed a statistically significant positive correlation between Treg cell infiltration and CXCL12 expression in HNSC, READ, SKCM



**FIGURE 7** Association between CXCL12 expression and overall survival (OS). **(A)** Forest plot of PFI,DSS,OS associations in 33 types of tumor. **(B)** Kaplan-Meier analysis of the association between CXCL12 expression and OS.

using multiple algorithms. Conversely, a negative correlation was observed between Th1 cell infiltration and CXCL12 expression in most tumor types. Scatterplot data demonstrated a positive correlation between CXCL12 expression in OV and infiltration by T cell CD4+ naive and memory as per the XCELL and CIBERSORT algorithm, and a negative correlation with T cell CD4+ Th1 infiltration as per the XCELL algorithm (Figures 14, 15).

### Immunohistochemical

Immunohistochemistry revealed markedly decreased CXCL12, IL17, STAT3 levels and elevated FOXP3 expression in 26 EAO samples compared with both EM and control endometrial tissue (Figure 16). Moreover, a reduced Th17/Treg ratio was seen in EAO ( $1.045 \pm 0.119$ ) as opposed to EM ( $0.951 \pm 0.100$ ) and controls ( $0.934 \pm 0.143$ ).

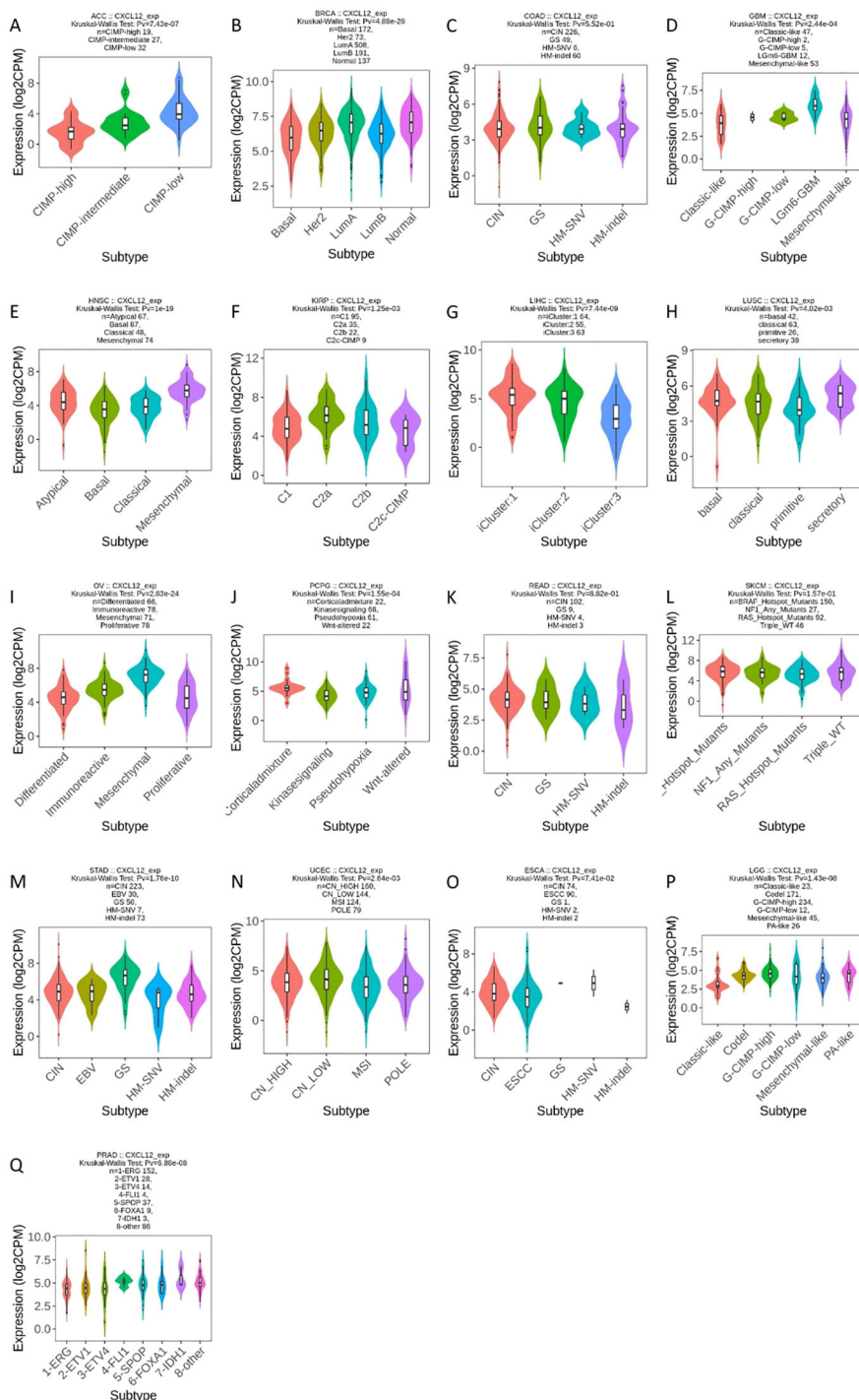


**FIGURE 8**

Correlations between CXCL12 expression and molecular subtypes in 17 cancers. **(A)** CIMP, CpG Island Methylator Phenotype; **(B)** Basal: ER-PR-Her2-, Her2: Her2+, LumA: ER+, LunB: ER+Her2+; **(C)** CIN, Chromosomal Instability; GS, Genomically Stable; HM-SNV, Hypermutated-Single Nucleotide Variant; HM-indel, Hypermutated-Insertion Deletion; **(D)** G-CIMP, Glioma-CpG island methylator phenotype; **(E)** HNSC, Head and Neck Squamous Cell Carcinoma; **(F)** KIRP, Kidney Papillary Rell Rarcinoma; **(G)** LIHC, Liver Hepatocellular Carcinoma; **(H)** LUSC, Lung Squamous Cell Carcinoma; **(I)** OV, Ovarian Cancer; **(J)** PCPG, Pheochromocytoma and Paraganglioma; **(K)** READ, Rectum Adenocarcinoma; CIN, Chromosomal Instability; GS, Genomically Stable; HM-SNV, Hypermutated-Single Nucleotide Variant; HM-INDEL, Hypermutated-Insertion Deletion; **(L)** SKCM, Skin Cutaneous Melanoma; **(M)** STAD, Stomach Adenocarcinoma; CIN, Chromosomal Instability; EBV, Epstein-Barr Virus; GS, Genomically Stable; HM-SNV, Hypermutated-Single Nucleotide Variant; HM-INDEL, Hypermutated-Insertion Deletion; **(N)** UCEC, Uterine Corpus Endometrial Carcinoma; CN-HIGH, Copy Number High; CN-LOW, Copy Number Low; MSI, Microsatellite Instability; POLE, Polymerase Epsilon; **(O)** ESCA, Esophageal Squamous Cell Carcinoma; CIN, Chromosomal Instability; ESCC, Esophageal Squamous Cell Carcinoma; GS, Genomically Stable; HM-SNV, Hypermutated-Single Nucleotide Variant; HM-INDEL, Hypermutated-Insertion Deletion; **(P)** LGG, Lower Grade Glioma; G-CIMP, Glioma CpG Island Methylator Phenotype; **(Q)** PRAD, Prostate Adenocarcinoma; ERG, Erythroblast Transformation-Specific Gene.

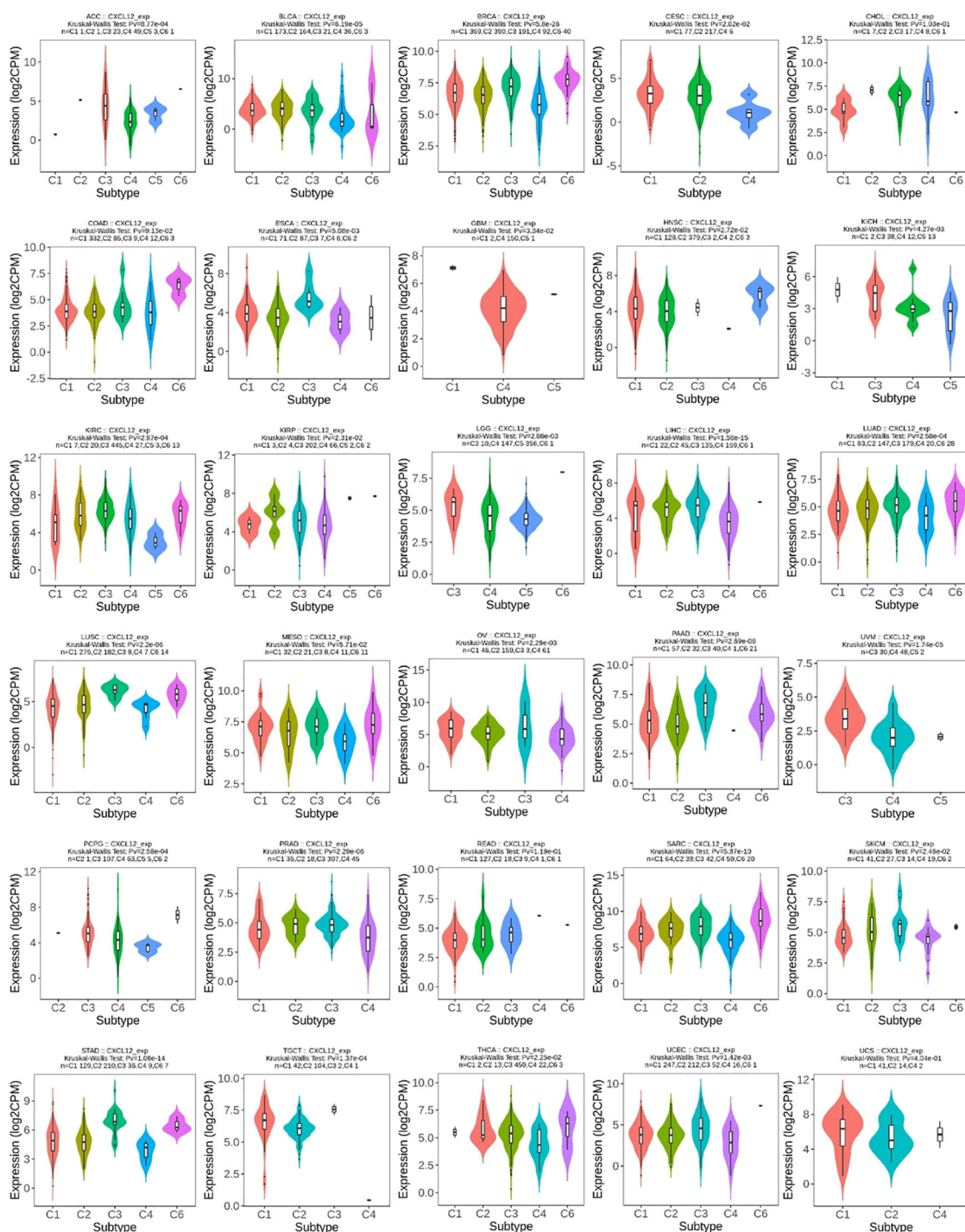


**FIGURE 9**  
Correlations between CXCL12 expression and immune subtypes in 30 cancers. C1 (wound healing), C2 (IFN- $\gamma$  dominant), C3 (inflammatory), C4 (lymphocyte deplete), C5 (immunologically quiet), and C6 (TGF- $\beta$  dominant).

## Discussion

Endometriosis, a women’s reproductive age disorder with ectopic endometrium growth, is linked to elevated rates of some malignancies, notably EAO. Although uncommon, ovarian cancer incidence escalates among endometriosis sufferers, primarily for

endometrioid and clear-cell types (13, 35). Autophagy is an essential process in cells, responsible for the recycling and degradation of damaged organelles or unwanted macromolecular complexes. It’s a highly conserved catabolic pathway evolutionarily speaking (36). There’s a complex link between endometriosis and ovarian cancer, with autophagy playing crucial roles in both conditions’



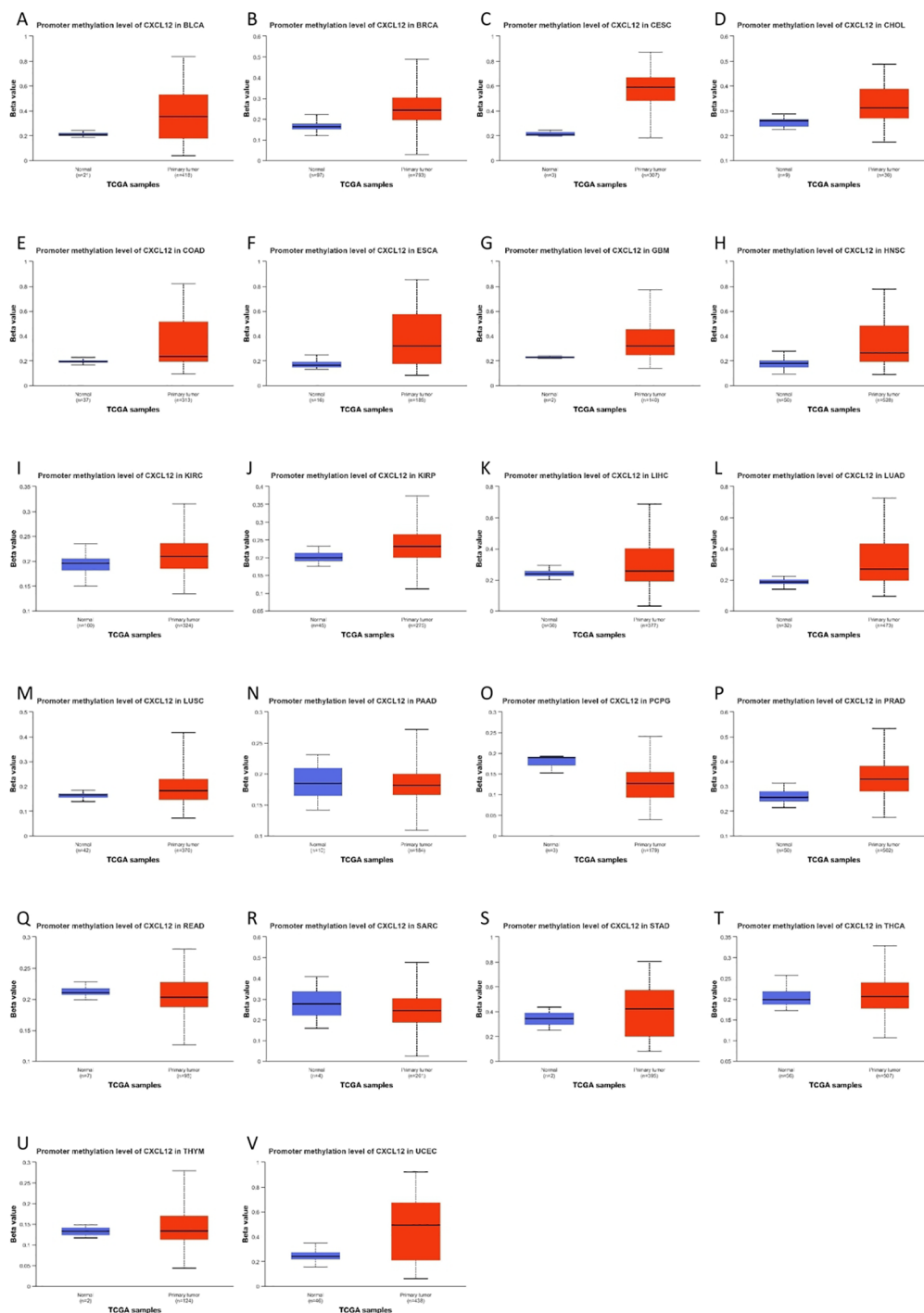


FIGURE 11  
The promoter methylation level of CXCL12 in cancers.

specificity (38). Aberrant expression of CXCL12/CXCR4 has been observed in diverse tumor types, and are believed to act as a crucial chemokine-chemokine receptor in promoting tumor growth. CXCL12 and CXCR4 have direct or indirect effects on tumor development. On one hand, CXCL12/CXCR4 stimulation initiates multiple signaling cascades regulating Ca<sup>2+</sup> flux, migration

transcription, and cellular viability (39). On the other hand, they affect tumor development through direct or indirect effects. The key role of CXCL12 and its receptor, CXCR4, is in regulating the accumulation of stromal and immune cells within the microenvironment (TME). This process leads to the formation of a specific immune microenvironment that significantly impacts

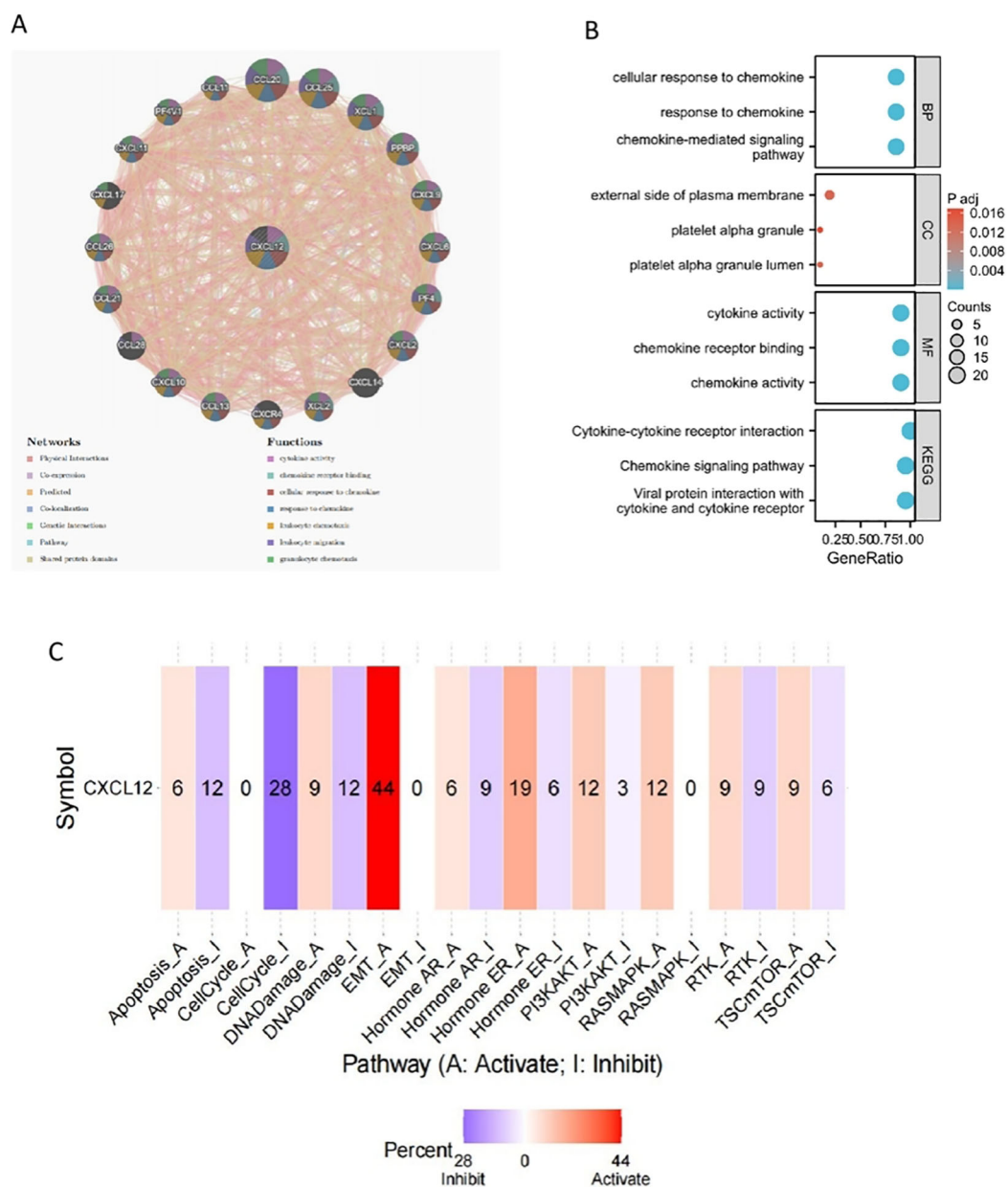
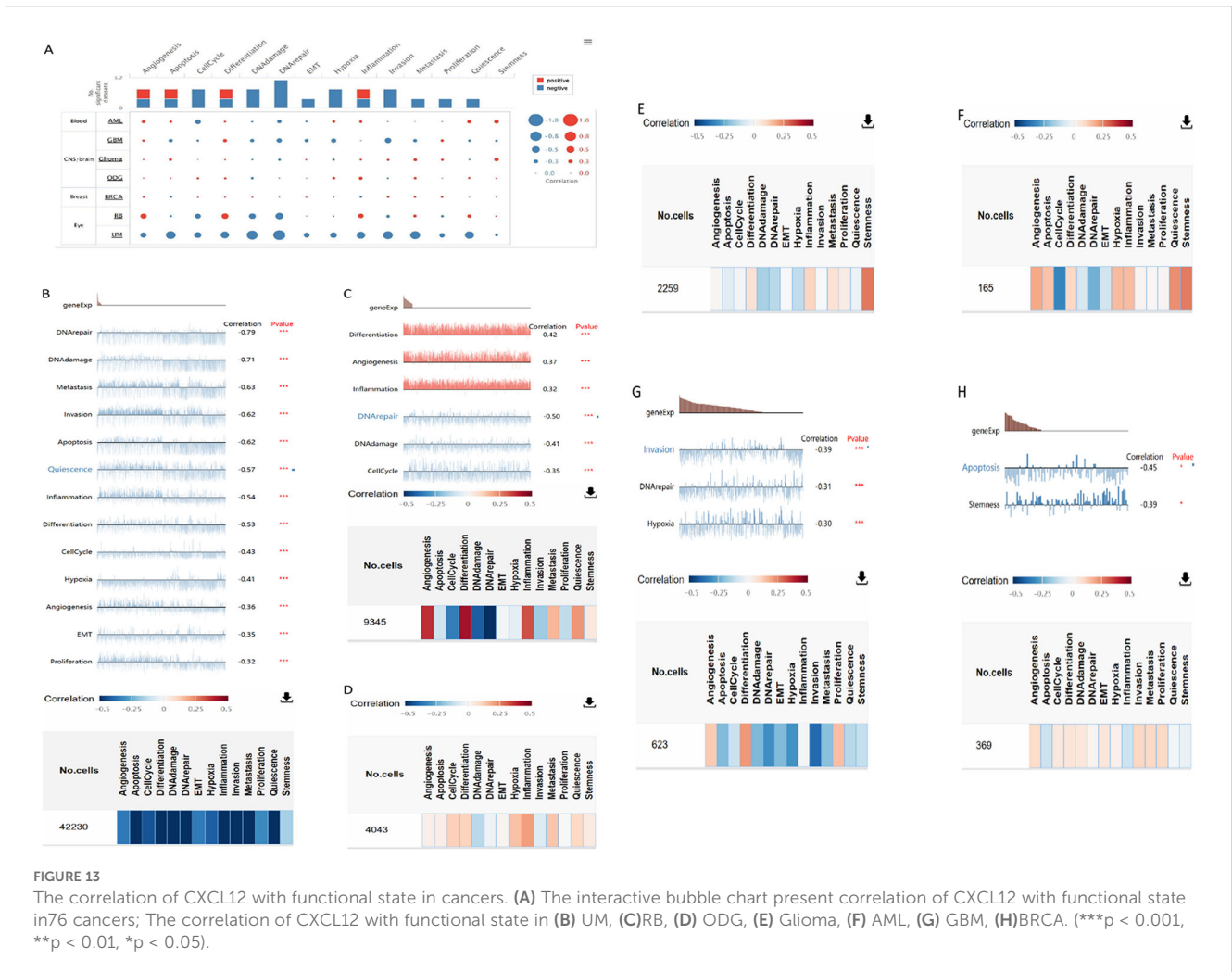


FIGURE 12 The gene-gene interaction network of CXCL12 from GeneMANIA; (B) GO/KEGG pathway enrichment for CXCL12 and closed interact genes; (C) CXCL12 with pathway activity or inhibition.

tumor growth, invasion, metastasis, angiogenesis, and drug resistance (40). The gene CXCL12, also recognized as stromal cell-derived factor 1 (SDF-1), resides on chromosome 10q11 of the human genome. It is widely expressed in different tissues and plays a crucial role in embryogenesis, angiogenesis, immune cell generation and recruitment of stem cells (41). CXCL12 has the ability to bind to both CXCR4 and CXCR7 receptors. Bioinformatic scrutiny revealed the pivotal role of CXCL12 in pan-cancer. Our

research assessed CXCL12 mRNA and protein levels in diverse human specimens, critically comparing these to cancerous states. We evaluated the diagnostic and predictive implications of CXCL12 expression in varied forms of cancer, together with delineating its variation in various immune cell subsets therein. CXCL12’s predominant variants and corresponding sites were pinpointed. PPI regulatory networks for CXCL12 were strategically designed, investigating its activation/inhibition mechanisms, revealing its



enriched functional pathways, and assessing its activity at a cellular level in select cancers. Lastly, a correlation study was performed examining CXCL12 expression and immune cell infiltration in multiple cancer types.

Cancer research is a prevailing theme in contemporary medicine. We used 33 cancer datasets from TCGA and CCLF platforms to uncover potential biomarkers for comprehensive cancer diagnosis via gene expression disparity analysis. The primary focus was on CXCL12, examined comprehensively within multiple cancers. This pan-cancer analysis revealed its substantial downregulation in numerous cancer types and its differing expression levels between malignant and healthy tissue. Its useful application for early detection, regulatory mechanisms, and associated genes were also discussed. Emerging evidence suggests a correlation between CXCL12 and disease states, notably tumors. The precise role of CXCL12 in tumorigenesis through shared molecular pathways requires further exploration. To our knowledge, no prior studies have conducted a pan-cancer analysis of CXCL12 across diverse tumor types.

Using the GTEx and TPA datasets, we conducted an evaluation of CXCL12 gene/protein expression across a range of tissues. Our analysis revealed a significant upregulation in adipose tissue, endometrium, spleen, smooth muscle, while showing inhibition in placental and cerebral cortex tissues. Additionally, investigating the pan-cancer context via unpaired sample analysis in the TCGA-GTEx dataset revealed a downregulated CXCL12 expression in cancerous tissues (e.g. BLCA, BRCA, CESC, etc.) compared to their corresponding normal counterparts. Conversely, it was elevated in DLBC, LAML, LGG, TGCT. No significant alterations were observed in GBM, PAAD, PCPG, or their corresponding normal tissues. Moving to the protein level, we conducted a thorough analysis of the CPTAC and HPA immunohistochemistry data, which indicated diminished CXCL12 protein expression in LUAD, UCEC, BRCA, KIRC, OV, LIHC, COAD, PAAD, HNSC. Furthermore, our analysis of the correlation between tumor stage and CXCL12 expression revealed a progressive decrease in CXCL12 expression in early stages (e.g. BLCA, STAD, LUAD, etc.) suggesting its potential role in early tumor detection.



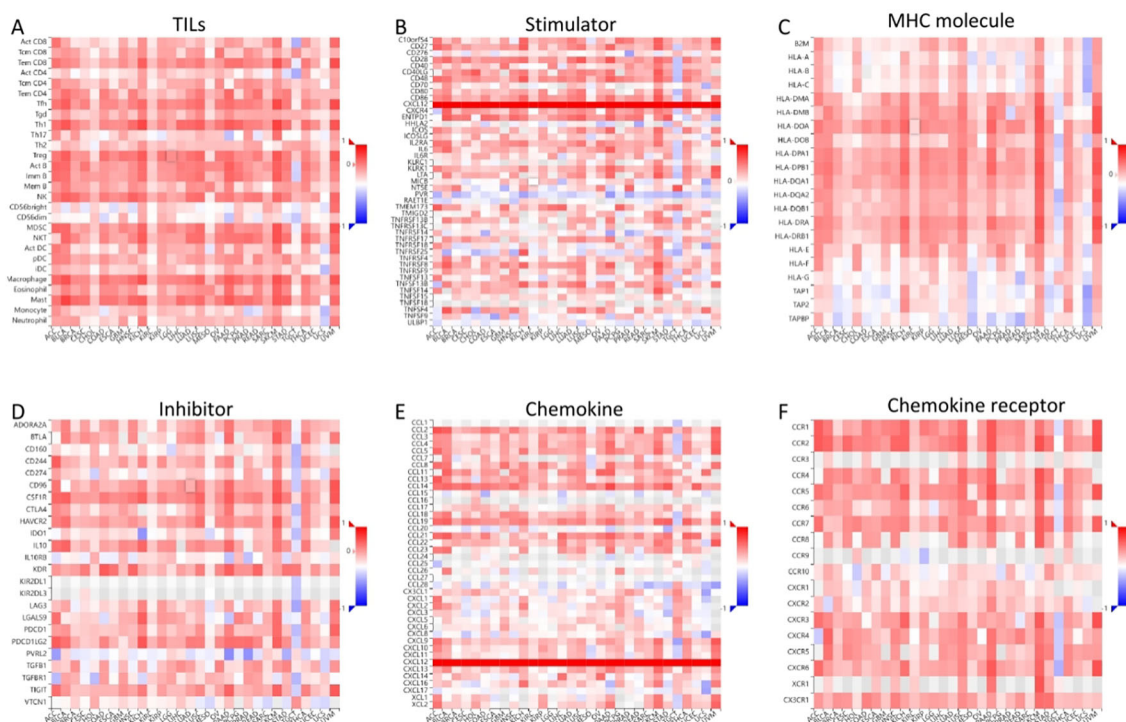


FIGURE 14

Correlation of CXCL12 with TILs and immunoregulation-related genes in 33 cancers. Correlations between CXCL12 expression and (A) TILs, (B) Immunostimulators, (C) MHC molecules, (D) Immunoinhibitors, (E) Chemokines, (F) Chemokine receptors. (\* $p < 0.05$ , \*\* $p < 0.01$ ).

With the advancement of research in tumor immunology, the concept of ‘tumor microenvironment’ has been introduced (42). This complex network consists of diverse cells, matrix surroundings, cytokines, vessels and lymphatic ducts, as well as tumor cell analysis and related physical factors. Together, these components shape the internal terrain of a tumor (43). This dynamic environment significantly impacts tumor initiation, progression, and metastasis. It has been reported that immune imbalance and chronic inflammation are significant contributors to cancer development (44). CD4+ T cells can differentiate into Th1, Th2, Treg, and Th17 subsets under different immune response stages, each with distinct biological functions. Th17 cells, a CD4+ T subset highly expressing interleukin-17 (IL-17), develop from naive CD4+ T cells via TGF- $\beta$  and IL-6 stimulation. As potent proinflammatory cells, they activate dendritic cells and T helper lymphocytes, induce various cytokines, perpetuate chronic inflammation, and contribute to carcinogenic microenvironments (45). Additionally, Th17 cells secrete IL-17, TNF- $\alpha$ , and IL-21, with IL-17 being an essential proinflammatory cytokine, inducing expression of other chemokines, proinflammatory cytokines, and metalloproteinases, thereby exacerbating inflammatory cell infiltration and tissue damage (46). Treg cells, derived from naive

CD4+ T cells independently by TGF- $\beta$ , are immunosuppressive cells that regulate immune response intensity, mitigate immune injury, mediate immune evasion through anti-tumor immune suppression, and promote tumor progression (47). Under certain conditions, Treg and Th17 cells reciprocally transform to maintain immune system stability, playing crucial roles in anti-tumor immunity. A growing body of evidence suggests that Th17/Treg cell ratio imbalance promotes inflammation and tumor progression (48). Our analysis indicates that Th17/Treg cell balance is crucial in understanding endometriosis-associated ovarian cancer (EAOC), leading us to collect formalin-fixed, paraffin-embedded (FFPE) samples of EAOC, EM, and normal endometrium for immunohistochemistry evaluations of CXCL12, FOXP3, STAT3, and IL17.

Despite the finding that CXCL12 expression and the ratio of Th17/Treg correlates with patient in EAOC, we were unable to demonstrate a direct impact of CXCL12 on patient through immune infiltration. Future research, targeting CXCL12 expression and immune infiltrates within a cancer demographic, may clarify these findings.

Despite integration of multi-database information, certain limitations existed within this research. Firstly, extensive microarray

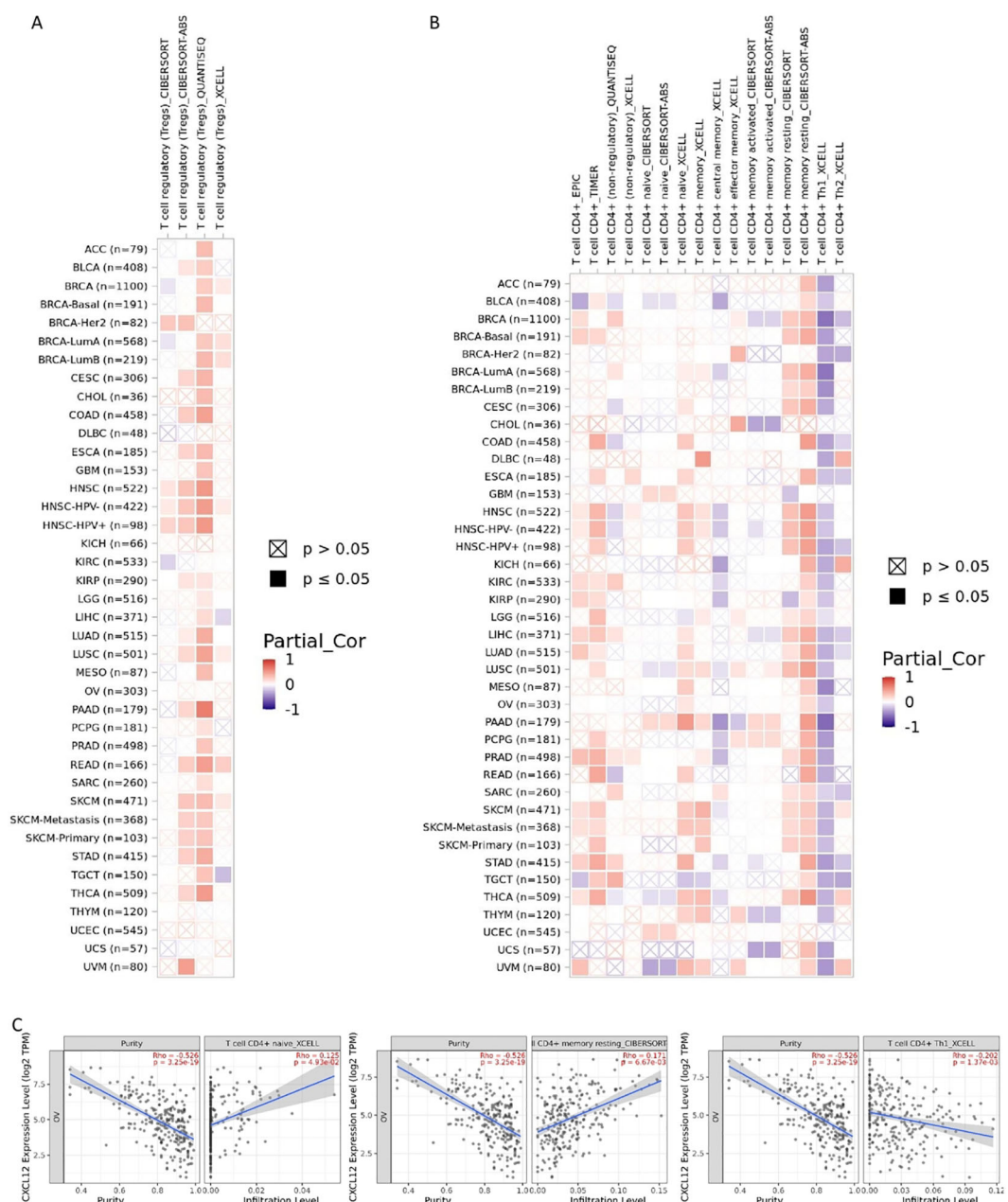


**FIGURE 15**  
Correlation analysis between CXCL12 expression and immune infiltration of Treg cell (A) and CD4+ T cell (B) across all types of cancer in TCGA. Different algorithms were used to explore the potential correlation between the expression level of the CXCL12 gene and the infiltration level of Treg cell and CD4+ T cell in OV (C).

and sequencing datasets analyzed primarily tumor tissue, potentially introducing bias during cell-level immune marker evaluations. To address this, high-resolution methodologies, like single cell RNA sequencing, are recommended. Secondly, lax attention was given to accurately representing CXCL12's posttranslational modifications in these databases. Indeed, both phosphorylation and ubiquitination can

alter CXCL12 functionality. Thirdly, conflicting data from disparate databases blur CXCL12's clear classification. This study exclusively examined computational CXCL12 expression-survival correlations across databases, excluding *in vivo/in vitro* experimentation. Such studies aimed at elucidating CXCL12's effects at cellular and molecular levels may assist understanding its role more effectively.

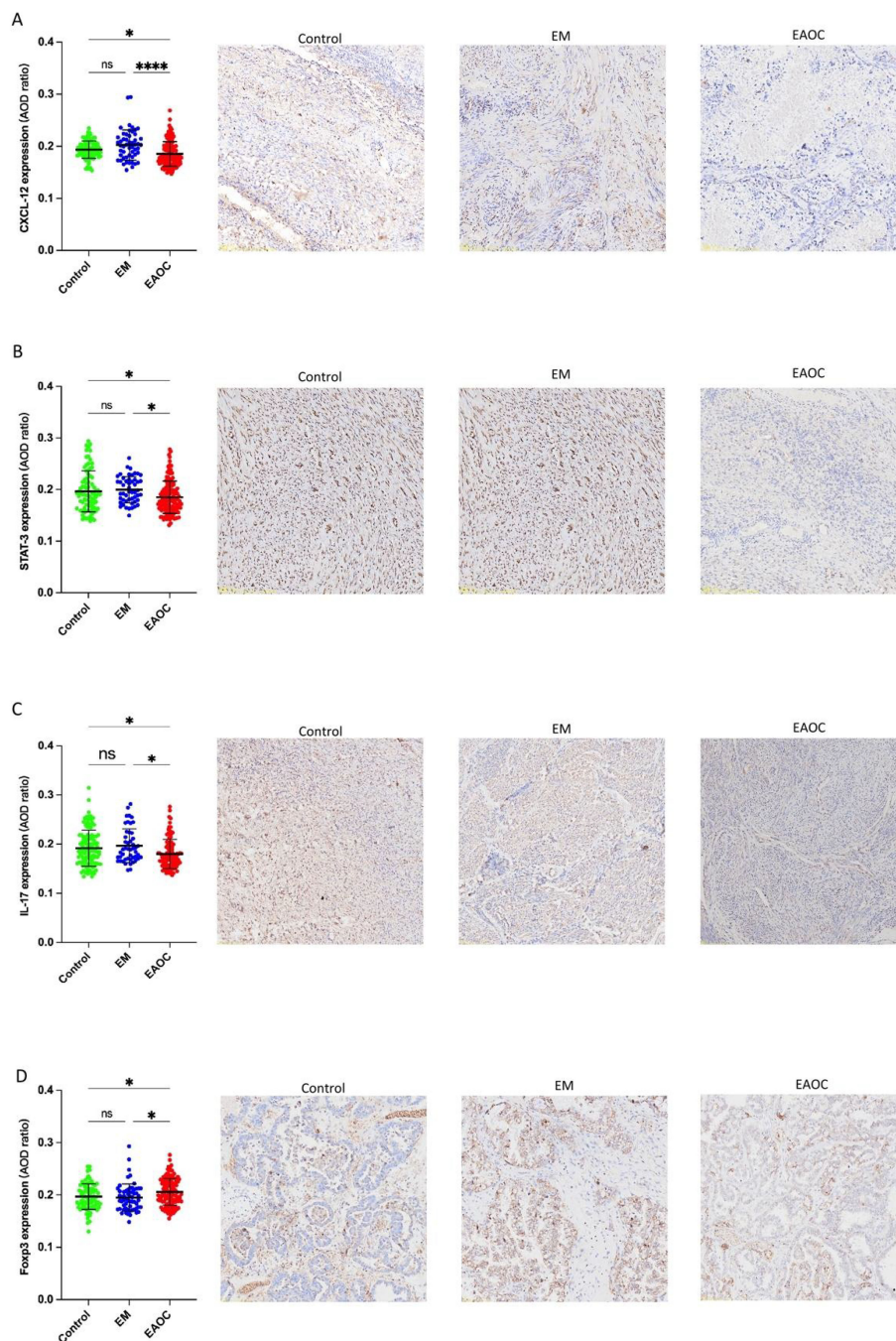


FIGURE 16 Expression of CXCL12 (A); STAT3 (B); IL-17 (C); FOXP3 (D) in EAO, EM and normal endometrium tissues.

## Conclusions

Our comprehensive investigations linked CXCL12 expression to prognosis, DNA methylation, immune cell influx, genetic alterations, and microsatellite stability across various cancers. These results offer crucial insights into CXCL12’s role in cancer initiation utilizing clinical tumor samples. Moreover, our analysis revealed substantial

CXCL12 expression differences between malignant and normal tissues, suggesting its potential correlation with prognosis. These findings indicate that CXCL12 is a distinct prognostic indicator in multiple tumors, necessitating further exploration due to divergent expression profiles across different tumor entities. Additionally, an unbalanced Th17/Treg cell ratio has been implicated in promoting inflammation and EAO progression concurrently.

## Data availability statement

The original contributions presented in the study are included in the article/supplementary material. Further inquiries can be directed to the corresponding author/s.

## Author contributions

MY: Data curation, Formal analysis, Methodology, Software, Visualization, Writing – original draft. SC: Writing – review & editing. ZL: Writing – review & editing. KW: Conceptualization, Funding acquisition, Project administration, Supervision, Writing – review & editing.

## Funding

The author(s) declare that financial support was received for the research and/or publication of this article. This work was supported

by the Natural Science Foundation of Sichuan Province (No. 2022NSFSC0790).

## Conflict of interest

The authors declare that the research was conducted in the absence of any commercial or financial relationships that could be construed as a potential conflict of interest.

## Publisher's note

All claims expressed in this article are solely those of the authors and do not necessarily represent those of their affiliated organizations, or those of the publisher, the editors and the reviewers. Any product that may be evaluated in this article, or claim that may be made by its manufacturer, is not guaranteed or endorsed by the publisher.

## References

- Murakami K, Kanto A, Sakai K, Miyagawa C, Takaya H, Nakai H, et al. Frequent PIK3CA mutations in eutopic endometrium of patients with ovarian clear cell carcinoma. *Modern pathology: an Off J United States Can Acad Pathology Inc.* (2021) 34:2071–9. doi: 10.1038/s41379-021-00861-3
- Bulun SE. Endometriosis. *New Engl J Med.* (2009) 360:268–79. doi: 10.1056/NEJMra0804690
- Seracchioli R, Ferrini G, Montanari G, Raimondo D, Spagnolo E, Di Donato N. Does laparoscopic shaving for deep infiltrating endometriosis alter intestinal function? A prospective study. *Aust New Z J obstetrics gynaecology.* (2015) 55:357–62. doi: 10.1111/ajo.12358
- Zafrakas M, Grimbizis G, Timologou A, Tarlatzis BC. Endometriosis and ovarian cancer risk: a systematic review of epidemiological studies. *Front Surg.* (2014) 1:14. doi: 10.3389/fsurg.2014.00014
- Raimondo D, Raffone A, Renzulli F, Sanna G, Raspollini A, Bertoldo L, et al. Prevalence and risk factors of central sensitization in women with endometriosis. *J minimally invasive gynecology.* (2023) 30:73–80.e71. doi: 10.1016/j.jmig.2022.10.007
- Scott RB. Malignant changes in endometriosis. *Obstetrics Gynecology.* (1953) 2:283–9.
- Kim HS, Kim TH, Chung HH, Song YS. Risk and prognosis of ovarian cancer in women with endometriosis: a meta-analysis. *Br J Cancer.* (2014) 110:1878–90. doi: 10.1038/bjc.2014.29
- Poole EM, Lin WT, Kvaskoff M, De Vivo I, Terry KL, Missmer SA. Endometriosis and risk of ovarian and endometrial cancers in a large prospective cohort of U.S. nurses. *Cancer causes control: CCC.* (2017) 28:437–45. doi: 10.1007/s10552-017-0856-4
- Pearce CL, Templeman C, Rossing MA, Lee A, Near AM, Webb PM, et al. Association between endometriosis and risk of histological subtypes of ovarian cancer: a pooled analysis of case-control studies. *Lancet Oncol.* (2012) 13:385–94. doi: 10.1016/s1470-2045(11)70404-1
- Hermens M, van Altna AM, Nieboer TE, Schoot BC, van Vliet HAAM, Siebers AG, et al. Incidence of endometrioid and clear-cell ovarian cancer in histological proven endometriosis: the ENOCA population-based cohort study. *Am J Obstet Gynecol.* (2020) 223:107.e101–107.e111. doi: 10.1016/j.ajog.2020.01.041
- Brinton LA, Gridley G, Persson I, Baron J, Bergqvist A. Cancer risk after a hospital discharge diagnosis of endometriosis. *Am J Obstet Gynecol.* (1997) 176:572–9. doi: 10.1016/S0002-9378(97)70550-7
- Brinton LA, Lamb EJ, Moghissi KS, Scoccia B, Althuis MD, Mabie JE, et al. Ovarian cancer risk associated with varying causes of infertility. *Fertility sterility.* (2004) 82:405–14. doi: 10.1016/j.fertnstert.2004.02.109
- Bastu E, Onder S, Demiral I, Ozurmeli M, Keskin G, Takmaz O, et al. Distinguishing the progression of an endometrioma: Benign or Malignant? *Eur J obstetrics gynecology Reprod Biol.* (2018) 230:79–84. doi: 10.1016/j.ejogrb.2018.09.026
- Bulun SE, Wan Y, Matei D. Epithelial mutations in endometriosis: link to ovarian cancer. *Endocrinology.* (2019) 160:626–38. doi: 10.1210/en.2018-00794
- Iwabuchi T, Yoshimoto C, Shigetomi H, Kobayashi H. Oxidative stress and antioxidant defense in endometriosis and its Malignant transformation. *Oxid Med Cell Longevity.* (2015) 2015:848595. doi: 10.1155/2015/848595
- Leenen S, Hermens M, de Vos van Steenwijk PJ, Bekkers RLM, van Esch EMG. Immunologic factors involved in the Malignant transformation of endometriosis to endometriosis-associated ovarian carcinoma. *Cancer immunology immunotherapy: CII.* (2021) 70:1821–9. doi: 10.1007/s00262-020-02831-1
- Suda K, Cruz Diaz LA, Yoshihara K, Nakaoka H, Yachida N, Motoyama T, et al. Clonal lineage from normal endometrium to ovarian clear cell carcinoma through ovarian endometriosis. *Cancer Sci.* (2020) 111:3000–9. doi: 10.1111/cas.14507
- El Hout M, Cosialls E, Mehrpour M, Hamaï A. Crosstalk between autophagy and metabolic regulation of cancer stem cells. *Mol Cancer.* (2020) 19:27. doi: 10.1186/s12943-019-1126-8
- Kobayashi H, Imanaka S, Yoshimoto C, Matsubara S, Shigetomi H. Molecular mechanism of autophagy and apoptosis in endometriosis: Current understanding and future research directions. *Reprod Med Biol.* (2024) 23:e12577. doi: 10.1002/rmb2.12577
- Nokhostin F, Azadehrah M, Azadehrah M. The multifaceted role and therapeutic regulation of autophagy in ovarian cancer. *Clin Trans oncology: Off Publ Fed Spanish Oncol Societies Natl Cancer Institute Mexico.* (2023) 25:1207–17. doi: 10.1007/s12094-022-03045-w
- Shin HY, Yang W, Chay DB, Lee EJ, Chung JY, Kim HS, et al. Tetraspanin 1 promotes endometriosis leading to ovarian clear cell carcinoma. *Mol Oncol.* (2021) 15:987–1004. doi: 10.1002/1878-0261.12884
- Suryawanshi S, Huang X, Elishaev E, Budiu RA, Zhang L, Kim S, et al. Complement pathway is frequently altered in endometriosis and endometriosis-associated ovarian cancer. *Clin Cancer research: an Off J Am Assoc Cancer Res.* (2014) 20:6163–74. doi: 10.1158/1078-0432.Ccr-14-1338
- Zhou G, Soufan O, Ewald J, Hancock REW, Basu N, Xia J. NetworkAnalyst 3.0: a visual analytics platform for comprehensive gene expression profiling and meta-analysis. *Nucleic Acids Res.* (2019) 47:W234–w241. doi: 10.1093/nar/gkz240
- Wang NN, Dong J, Zhang L, Ouyang D, Cheng Y, Chen AF, et al. HAMdb: a database of human autophagy modulators with specific pathway and disease information. *J cheminformatics.* (2018) 10:34. doi: 10.1186/s13321-018-0289-4
- Fonseka P, Pathan M, Chitti SV, Kang T, Mathivanan S. FunRich enables enrichment analysis of OMICS datasets. *J Mol Biol.* (2021) 433:166747. doi: 10.1016/j.jmb.2020.166747
- Warde-Farley D, Donaldson SL, Comes O, Zuberi K, Badrawi R, Chao P, et al. The GeneMANIA prediction server: biological network integration for gene

- prioritization and predicting gene function. *Nucleic Acids Res.* (2010) 38:W214–220. doi: 10.1093/nar/gkq537
27. Szklarczyk D, Kirsch R, Koutrouli M, Nastou K, Mehryary F, Hachilif R, et al. The STRING database in 2023: protein-protein association networks and functional enrichment analyses for any sequenced genome of interest. *Nucleic Acids Res.* (2023) 51:D638–d646. doi: 10.1093/nar/gkac1000
28. Chandrashekar DS, Karthikeyan SK, Korla PK, Patel H, Shovon AR, Athar M, et al. UALCAN: An update to the integrated cancer data analysis platform. *Neoplasia (New York N.Y.)*. (2022) 25:18–27. doi: 10.1016/j.neo.2022.01.001
29. Uhlén M, Fagerberg L, Hallström BM, Lindskog C, Oksvold P, Mardinoglu A, et al. Proteomics. Tissue-based map of the human proteome. *Sci (New York N.Y.)*. (2015) 347:1260419. doi: 10.1126/science.1260419
30. Raffone A, Raimondo D, Neola D, Travaglino A, Raspollini A, Giorgi M, et al. Diagnostic accuracy of ultrasound in the diagnosis of uterine leiomyomas and sarcomas. *J minimally invasive gynecology*. (2024) 31:28–36.e21. doi: 10.1016/j.jmig.2023.09.013
31. Hanley JA, McNeil BJ. The meaning and use of the area under a receiver operating characteristic (ROC) curve. *Radiology*. (1982) 143:29–36. doi: 10.1148/radiology.143.1.7063747
32. Ru B, Wong CN, Tong Y, Zhong JY, Zhong SSW, Wu WC, et al. TISIDB: an integrated repository portal for tumor-immune system interactions. *Bioinf (Oxford England)*. (2019) 35:4200–2. doi: 10.1093/bioinformatics/btz210
33. Liu CJ, Hu FF, Xia MX, Han L, Zhang Q, Guo AY. GSCALite: a web server for gene set cancer analysis. *Bioinf (Oxford England)*. (2018) 34:3771–2. doi: 10.1093/bioinformatics/bty411
34. Cerami E, Gao J, Dogrusoz U, Gross BE, Sumer SO, Aksoy BA, et al. The cBio cancer genomics portal: an open platform for exploring multidimensional cancer genomics data. *Cancer Discovery*. (2012) 2:401–4. doi: 10.1158/2159-8290.Cd-12-0095
35. Centini G, Schettini G, Pieri E, Giorgi M, Lazzeri L, Martire FG, et al. Endometriosis-related ovarian cancer: where are we now? A narrative review towards a pragmatic approach. *J Clin Med*. (2024) 13. doi: 10.3390/jcm13071933
36. Nie T, Zhu L, Yang Q. The classification and basic processes of autophagy. *Adv Exp Med Biol*. (2021) 1208:3–16. doi: 10.1007/978-981-16-2830-6\_1
37. Shen HH, Zhang T, Yang HL, Lai ZZ, Zhou WJ, Mei J, et al. Ovarian hormones-autophagy-immunity axis in menstruation and endometriosis. *Theranostics*. (2021) 11:3512–26. doi: 10.7150/thno.55241
38. Cambier S, Gouwy M, Proost P. The chemokines CXCL8 and CXCL12: molecular and functional properties, role in disease and efforts towards pharmacological intervention. *Cell Mol Immunol*. (2023) 20:217–51. doi: 10.1038/s41423-023-00974-6
39. Yang Y, Li J, Lei W, Wang H, Ni Y, Liu Y, et al. CXCL12-CXCR4/CXCR7 axis in cancer: from mechanisms to clinical applications. *Int J Biol Sci*. (2023) 19:3341–59. doi: 10.7150/ijbs.82317
40. Lu L, Li J, Jiang X, Bai R. CXCR4/CXCL12 axis: "old" pathway as "novel" target for anti-inflammatory drug discovery. *Medicinal Res Rev*. (2024) 44:1189–220. doi: 10.1002/med.22011
41. Anastasiadou DP, Quesnel A, Duran CL, Filippou PS, Karagiannis GS. An emerging paradigm of CXCL12 involvement in the metastatic cascade. *Cytokine Growth factor Rev*. (2024) 75:12–30. doi: 10.1016/j.cytogfr.2023.10.003
42. Pitt JM, Marabelle A, Eggermont A, Soria JC, Kroemer G, Zitvogel L. Targeting the tumor microenvironment: removing obstruction to anticancer immune responses and immunotherapy. *Ann oncology: Off J Eur Soc Med Oncol*. (2016) 27:1482–92. doi: 10.1093/annonc/mdw168
43. Xiao Y, Yu D. Tumor microenvironment as a therapeutic target in cancer. *Pharmacol Ther*. (2021) 221:107753. doi: 10.1016/j.pharmthera.2020.107753
44. Denk D, Greten FR. Inflammation: the incubator of the tumor microenvironment. *Trends Cancer*. (2022) 8:901–14. doi: 10.1016/j.trecan.2022.07.002
45. Marques HS, de Brito BB, da Silva FAF, Santos MLC, de Souza JCB, Correia TML, et al. Relationship between Th17 immune response and cancer. *World J Clin Oncol*. (2021) 12:845–67. doi: 10.5306/wjco.v12.i10.845
46. Knochelmann HM, Dwyer CJ, Bailey SR, Amaya SM, Elston DM, Mazza-McCrann JM, et al. When worlds collide: Th17 and Treg cells in cancer and autoimmunity. *Cell Mol Immunol*. (2018) 15:458–69. doi: 10.1038/s41423-018-0004-4
47. Togashi Y, Shitara K, Nishikawa H. Regulatory T cells in cancer immunosuppression - implications for anticancer therapy. *Nat Rev Clin Oncol*. (2019) 16:356–71. doi: 10.1038/s41571-019-0175-7
48. Qianmei Y, Zehong S, Guang W, Hui L, Lian G. Recent advances in the role of Th17/Treg cells in tumor immunity and tumor therapy. *Immunologic Res*. (2021) 69:398–414. doi: 10.1007/s12026-021-09211-6